

Integrated species delimitation and conservation implications of an endangered weevil *Pachyrhynchus sonani* (Coleoptera: Curculionidae) in Green and Orchid Islands of Taiwan

YEN-TING CHEN¹, HUI-YUN TSENG^{2,3}, MING-LUEN JENG³,
YONG-CHAO SU^{4,5}, WEN-SAN HUANG³ and CHUNG-PING LIN¹ 

¹Department of Life Science, National Taiwan Normal University, Taipei, Taiwan, ²Department of Life Science, Tunghai University, Taichung, Taiwan, ³Department of Biology, National Museum of Natural Science, Taichung, Taiwan, ⁴Biodiversity Institute and Department of Ecology and Evolutionary Biology, University of Kansas, Lawrence, KS, U.S.A. and ⁵Department of Biomedical Science and Environmental Biology, Kaohsiung Medical University, Kaohsiung, Taiwan

Abstract. Oceanic islands are productive habitats for generating new species and high endemism, which is primarily due to their geographical isolation, smaller population sizes and local adaptation. However, the short divergence times and subtle morphological or ecological divergence of insular organisms may obscure species identity, so the cryptic endemism on islands may be underestimated. The endangered weevil *Pachyrhynchus sonani* Kôno (Coleoptera: Curculionidae: Entiminae: Pachyrhynchini) is endemic to Green Island and Orchid Island of the Taiwan-Luzon Archipelago and displays widespread variation in coloration and host range, thus raising questions regarding its species boundaries and degree of cryptic diversity. We tested the species boundaries of *P. sonani* using an integrated approach that combined morphological (body size and shape, genital shape, coloration and cuticular scale), genetic (four genes and restriction site-associated DNA sequencing, RAD-seq) and ecological (host range and distribution) diversity. The results indicated that all the morphological datasets for male *P. sonani*, except for the colour spectrum, reveal overlapping but statistically significant differences between islands. In contrast, the morphology of the female *P. sonani* showed minimum divergence between island populations. The populations of *P. sonani* on the two islands were significantly different in their host ranges, and the genetic clustering and phylogenies of *P. sonani* established two valid evolutionary species. Integrated species delimitation combining morphological, molecular and ecological characters supported two distinct species of *P. sonani* from Green Island and Orchid Island. The Green Island population was described as *P. jitanasaius* **sp.n.** Chen & Lin, and it is recommended that its threatened conservation status be recognized. Our findings suggest that the inter-island speciation of endemic organisms inhabiting both islands may be more common than previously thought, and they highlight the possibility that the cryptic diversity of small oceanic islands may still be largely underestimated.

Correspondence: Chung-Ping Lin, Department of Life Science, National Taiwan Normal University, No. 88, Sec. 4, Tingzhou Road, Taipei, 11610, Taiwan. E-mail: treehopper@ntnu.edu.tw; Wen-San Huang, Department of Biology, Amphibians and Reptiles Section, National Museum of Natural Science, No. 1, Guancian Road, Taichung, 40453, Taiwan. E-mail: wshuang@mail.nmns.edu.tw

Introduction

Oceanic archipelagos are one of the most productive arenas on the earth for the generation of new species and high endemism (Grant, 1998; Gillespie & Roderick, 2002). Their geographical isolation, together with the geological and ecological dynamics of islands, greatly facilitates *in situ* speciation and subsequent diversification in these remote habitats (MacArthur & Wilson, 1967; Heaney, 2000; Whittaker *et al.*, 2008). Neighbouring islands of a given oceanic archipelago often harbour different but closely related species because of geographical proximity, limited dispersal and sexual or ecological divergence caused by local adaptation. For example, the classic studies of Darwin's finches of the Galápagos Islands (Grant & Grant, 2014), the *Anolis* lizards of the Caribbean islands (Losos, 2009) and the fauna of the Hawaiian islands (Wagner & Funk, 1995) all demonstrate the enormous adaptive radiation and rapid diversification of closely related island organisms. However, short divergence times and limited phenotypic divergence of endemic insular organisms may obscure species identity, so the cryptic endemism may be underestimated on islands (Bickford *et al.*, 2007).

Pachyrhynchus (Germar) weevils (Coleoptera: Curculionidae: Entiminae: Pachyrhynchini) arguably exhibit the most diverse and spectacular colour radiation of all of the terrestrial organisms of the Old World tropics (Wallace, 1895; Schultze, 1923), and this remarkable array of coloration was found to be a result of light interference by a three-dimensional photonic polycrystal structure within the cuticular scale of the exoskeleton (Welch *et al.*, 2007; McNamara *et al.*, 2013). The bright colours of *Pachyrhynchus* function as aposematic signals that deter attacks by lizard predators (Tseng *et al.*, 2014). These flightless *Pachyrhynchus* weevils have the highest species diversity in the Philippine archipelago and adjacent oceanic islands (approximately 108 recognized species; Schultze, 1923; Yoshitake, 2012; Bollino & Sandel, 2015). Approaching their northern boundary of distribution, *Pachyrhynchus* inhabits a few remote volcanic islands of the Taiwan-Luzon Archipelago, which extends from Luzon to Okinawa and includes Green Island (Lyudao) and Orchid Island (Lanyu) located offshore of southeastern Taiwan (Kano, 1929; Kôno, 1930; Starr & Wang, 1992) (Fig. 1a). Green Island and Orchid Island were created by volcanic uplift of submarine arc approximately 2–3 Ma (Green Island, 2.0 to 0.54 Ma; Orchid Island, 3.5 to 1.4 Ma; Yang *et al.*, 1996). Five currently recognized Taiwanese species of *Pachyrhynchus* are distributed on Green and Orchid islands, including *P. insularis* Kano, *P. sarcitis kotoensis* Kôno, *P. sonani* Kôno, *P. tobafolius* Kano and *P. yamianus* Kano. Except for the rare endemic *P. insularis* of Orchid Island, the other four *Pachyrhynchus* species occur on both Green and Orchid islands but differ in their relative abundance. *Pachyrhynchus sarcitis kotoensis*, *P. tobafolius* and *P. yamianus* are more populous on Orchid Island than on Green Island, whereas *P. sonani* is more abundant on Green Island (Starr & Wang, 1992).

In 2009 the Wildlife Conservation Act of Taiwan officially listed all five of the endemic *Pachyrhynchus* species of Green and Orchid islands as Category II protected species (i.e. rare

and valuable species) (Chao *et al.*, 2009). The criteria used to assess their threat categories were mainly based on the level of endemism, collection pressure and habitat loss, but in addition to the commonly applied criteria described earlier, systematic and phylogenetic information based on ecological, morphological and molecular data can provide essential information for identifying distinct evolutionary lineages, delimiting species boundaries and setting conservation strategies and priorities (reviewed in Pellens & Grandcolas, 2016). This knowledge is especially important for cryptic species and complexes of endangered species, which may consist of multiple unrecognized species that are even rarer than the nominal species (Bickford *et al.*, 2007; Wiens, 2007). At present, the five Taiwanese *Pachyrhynchus* species are primarily distinguished by body size and shape and by the variation in the brightly coloured spots and stripes decorating their thoraces, legs and elytra (Fig. 1b, d) (Kano, 1929; Kôno, 1930). Although the aposematic coloration of a particular *Pachyrhynchus* species may have been subject to strong stabilizing selection to minimize deviation from its effective predator-detering colour pattern (Tseng *et al.*, 2014), a cursory examination of available *P. sonani* specimens revealed widespread colour differences between and within island populations (Fig. 1e). For example, the posterior-lateral elytrous stripes of *P. sonani* from Orchid Island are elongate, whereas the *P. sonani* from Green Island have reduced, small spherical spots (Fig. 1e, character 6). In addition to colour variation, the available host plant records for *P. sonani* reveal variable host plant ranges that characterize the populations of each island. *Pachyrhynchus sonani* frequently occurs on the sea poison tree, *Barringtonia asiatica* (Lecythidaceae), on Orchid Island, but on Green Island, it is often found on Ceylon ardisia, *Ardisia elliptica* (Primulaceae). Therefore, the variable colour pattern and host plant range of *P. sonani* raise questions regarding its species boundaries and the number of cryptic species among the populations of the islands.

This study aimed to test the species boundaries of *P. sonani* from Green Island and Orchid Island using an integrated approach combining characters of phenotypic, genetic and ecological diversity. A sympatric and congeneric species, *P. tobafolius* (Fig. 1b), that shows minimal between-island variation in colour and host range was simultaneously analysed for comparison using multiple character datasets. First, we analysed multiple phenotypic traits, including the body size and shape, genital shape, coloration and cuticular scales from the two island populations of *P. sonani*. Second, we reconstructed phylogenies and tested for genetic differentiation between the island populations of *P. sonani* using two molecular datasets, four gene sequences and a genome-wide sample of single nucleotide polymorphisms (SNPs) generated from restriction site-associated DNA (RAD) sequencing. Third, we quantified the level of ecological differentiation in host plant range between the island populations of *P. sonani*. The recently developed Bayesian species delimitation method of integrating multiple morphological, genetic and ecological traits can improve the accuracy of estimated species boundaries that only use genetic data (Edwards & Knowles, 2014; Solís-Lemus *et al.*, 2015). Finally, we estimated the *P. sonani*

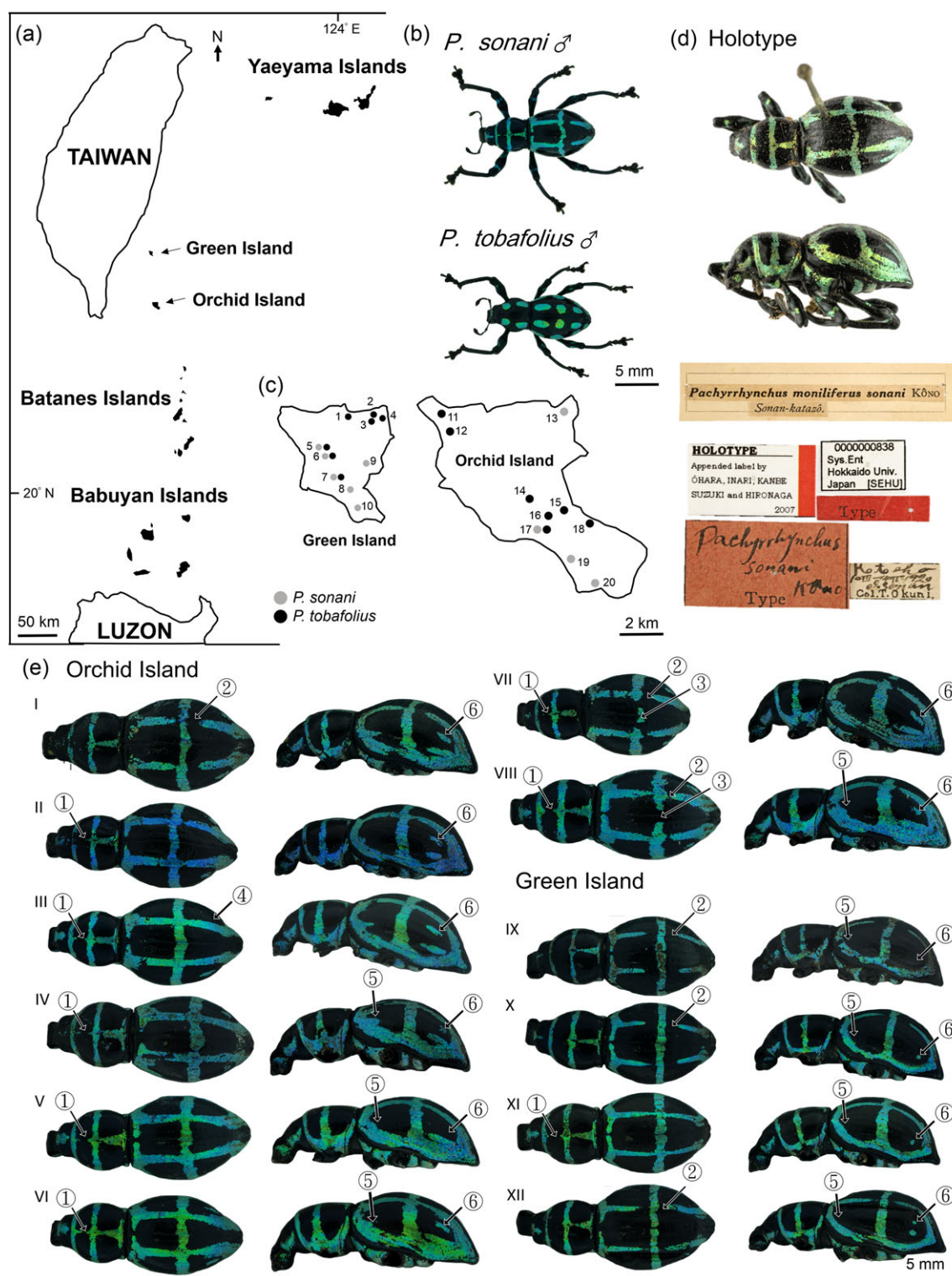


Fig. 1. Map of Green Island and Orchid Island (a) inhabited by *Pachyrhynchus sonani* and *Pachyrhynchus tobaefolius* (b). (c) Sampling sites (numbers refer to Appendix S1). (d) Holotype of *Pachyrhynchus sonani* (Kôno, 1930) (*Pachyrhynchus moniliferus sonani* is a synonym). Images obtained with permission from the Center of Digital Collections Research and Development, National Taiwan University. (e) Geographic variation in the coloration of *Pachyrhynchus sonani*. [Colour figure can be viewed at wileyonlinelibrary.com].

species boundary by integrating the characters of phenotypic, genetic and ecological diversity under a Bayesian coalescent framework in INTEGRATED BAYESIAN PHYLOGENETICS AND PHYLOGEOGRAPHY (iBPP) (Solís-Lemus *et al.*, 2015). Our integrated species delimitation results provide sufficient evidence for recognizing the population of *P. sonani* from Green Island as a distinct species. Based on these results we present the taxonomic description of a new species, *Pachyrhynchus jitanasaius* sp.n. Chen & Lin.

Materials and methods

Insect sampling and preparation

We collected weevils by hand or with insect nets from 20 sites on Green Island (22°39'49" N, 121°29'24" E) and Orchid Island (22°03'49" N, 121°32'41" E) between April 2006 and August 2014 (Fig. 1c, Appendix S1); the specimens were preserved in 95% ethanol (EtOH) after capture. The host plant species were identified by references (Huang & Wu, 1998), and the weevils were associated with the host plants either by the presence of the insects on the plants or by observing them feeding on the leaves and bark. We dissected the weevils to separate the legs and the genitalia. The genitalia were bathed in 15% KOH at 70°C for 15 min to clear the structure and were then kept in 50% glycerine for photographs and illustrations, and the thoracic muscles and legs were preserved in 95% EtOH in a -20°C freezer for subsequent molecular analyses. The insect bodies were secured with insect pins on a Styrofoam plate and oven-dried at 50°C for 72 h; they were also used later for photographs. All voucher specimens of this study were deposited in the insect collection of the National Museum of Natural Science (NMNS), Taichung, Taiwan.

Morphometric analyses

The dorsal and lateral body (Fig. 2a, b), lateral aedeagus (Fig. 2c) and ventral sternite VIII of the female genitalia (Fig. 2d) were photographed using a digital camera (EOS700D, Canon, Tokyo, Japan) mounted on a stereo microscope (SZ61, Olympus, Tokyo, Japan) at 10–45× with a single white light projected from above at an angle of 45°. The camera and the specimens were manually adjusted to be parallel to each other. A ruler with minimum gradation of 1.0 mm was placed by the specimen for calibration of the images. The photographs were saved in JPEG format (300 dpi) and then imported into TPSDIG2 (Rohlf, 2005). Twelve measurements of body shape [rostrum width (RW), head width (HW), thorax width (TW), abdomen width (AW), rostrum length (RL), head length (HL), thorax length (TL), abdomen length (AL), rostrum height (RH), head height (HH), thorax height (TH) and abdomen height (AH)] (Fig. 2a, b) were obtained by analysing the photographs using the ruler tool in PHOTOSHOP CS5 (Adobe Systems Inc., San Jose, CA, U.S.A.). Each of the morphological structures were photographed three times to calculate the measurement

error (%ME) by comparing the variation within and between individuals using the formula developed by Bailey & Byrnes (1990): $\%ME = [S_{within}^2 / (S_{within}^2 + S_{among}^2)] \times 100\%$, where $S_{within}^2 = ME_{within}$, and $S_{among}^2 = (ME_{among} + ME_{within})/3$. ME_{within} and ME_{among} are the within-individual and between-individual mean sums of squares of a Model II ANOVA, and the measurement errors of the morphological structures were 6.58% for the body ($n=92$), 5.15% for the aedeagus ($n=59$), and 1.50% for the female genitalia ($n=22$). The significance of the measurement differences between island weevil populations was analysed using multivariate analysis of covariance (MANCOVA) in SPSS v. 17.0 (Norris, 2005). The difference in genital size [male, distance between landmark 1 and 12 of the aedeagus (Fig. 2c); female, distance between landmark two and three of the sternite VIII (Fig. 2d)] was analysed using a *t*-test in SPSS.

Eleven and ten body landmarks located dorsally and laterally, respectively, were identified to describe the body shape of the weevils (Fig. 2a, b). Twelve landmarks were chosen to characterize the aedeagus, including two landmarks located at the apex and base (Fig. 2c, nos 1 and 12) and ten semi-landmarks (Fig. 2c, nos 2–11), which were generated by crossing the inner and outer edges of the aedeagus with each of ten radii spaced 30° apart, beginning from the midpoint between landmark nos 1 and 12. Five landmarks were selected to describe the ventral sternite VIII of the female genitalia (Fig. 2d). The coordinates of all the landmark locations were transformed into eigenvectors using general Procrustes analysis (GPA) (Rohlf & Slice, 1990) in COORDGEN6H of the Integrated Morphometric Package (IMP) (Sheets, 2004), and the eigenvectors were summarized using principal component analysis (PCA) in PCAGEN6P of the IMP. The resulting first and second principal components (PCs) and eigenvectors were analysed using MANCOVA in SPSS to test the significance of the difference in the body shape between the populations of the two islands. The shape variables (uniform components and partial warps) of the body and genitals were treated as dependent fixed variables, and the centroid size was used as a covariate. Goodall's *F*-test (Anderson, 1984) was employed to test the significance of the differences in the body and genital shape eigenvectors between island populations using TWOGROUP6H of the IMP. Thin-plate spline deformation grids were generated between the consensus of the two populations in PCAGEN6P to visualize the level and location of the variations in the body and genital shapes.

Coloration and cuticular scale

We quantified the colour of the weevils by measuring the reflectance spectrum of a pre-defined surface area (0.785 mm² at the lateral-posterior end of the left elytra; Fig. 2b, circle d) located within the colour stripe at a distance of 1.0 mm using a spectrometer (detection range, 250–800 nm; Jaz spectrometer; Ocean Optics, FL, U.S.A.), which was connected to a reflection probe (ZFQ-13101) with a deuterium–tungsten halogen light source (DH-2000-BAL). A diffuse reflectance standard (WS-1-SL) was used for calibration in SpectraSuite (Ocean

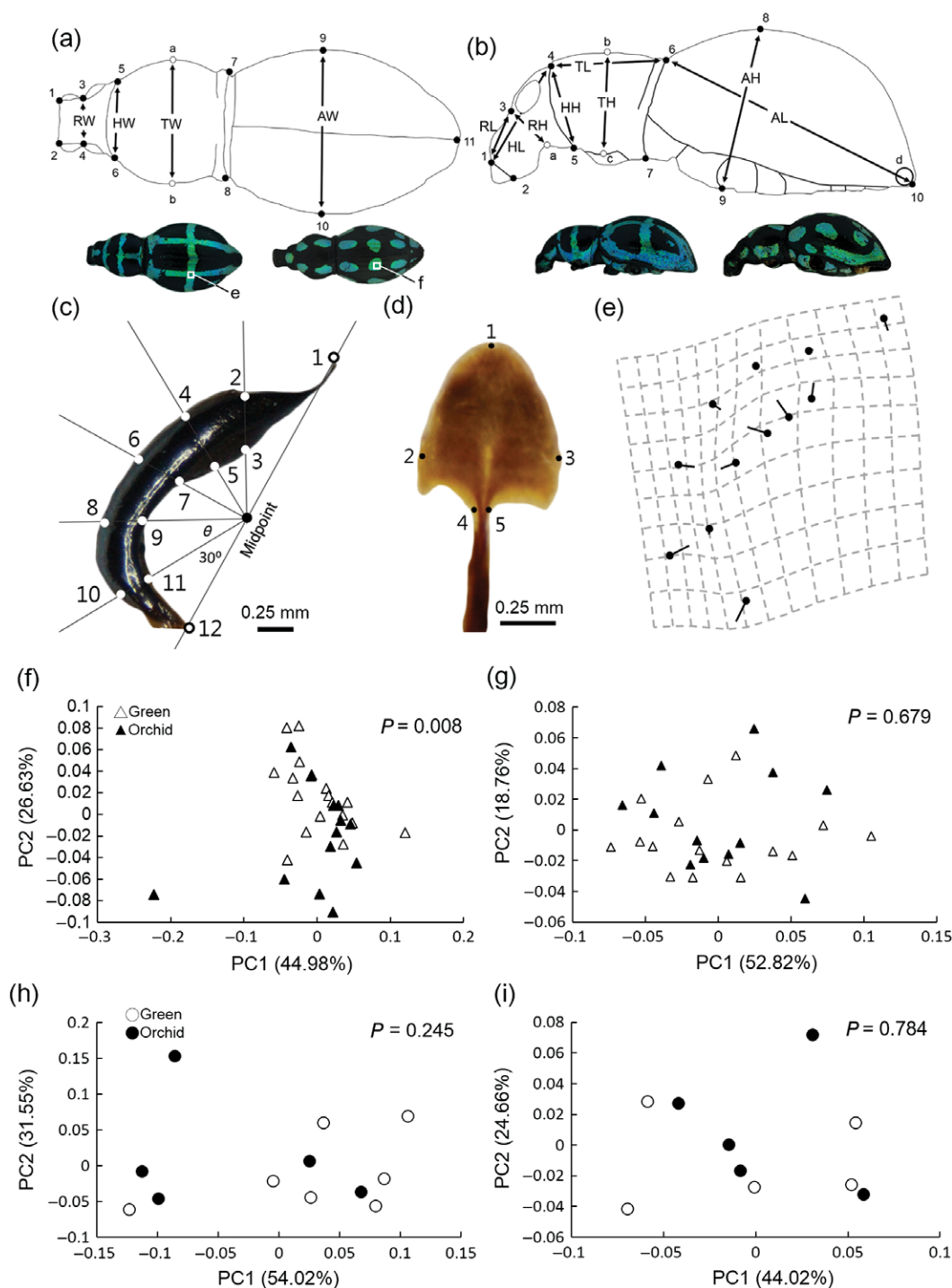


Fig. 2. Location of 11 dorsal (a) and ten lateral (b) landmarks used to define the body shapes of *Pachyrhynchus* weevils. Circle 'd' is the location for measuring the colour spectrum of the scales, and rectangles 'e' and 'f' are the locations for calculating the number and types of scales on *Pachyrhynchus sonani* and *Pachyrhynchus tobafolius*, respectively. RW, rostrum width; HW, head width; TW, thorax width; AW, abdomen width; RL, rostrum length; HL, head length; TL, thorax length; AL, abdomen length; RH, rostrum height; HH, head height; TH, thorax height; AH, abdomen height. (c) Location of two landmarks and ten semi-landmarks for aedeagus (lateral view). The size of the aedeagus was measured between landmarks 1 and 12. (d) Location of five female sternite VIII landmarks (ventral view), the sizes of which were measured between landmarks 1 and 12. (e) Aedeagus shape deformation grid from the Orchid to Green Island populations of *Pachyrhynchus sonani* (4×). Morphometric analyses of the aedeagus (f, g) and sternite VIII shapes (h, i) of *P. sonani* and *P. tobafolius*. [Colour figure can be viewed at wileyonlinelibrary.com.]

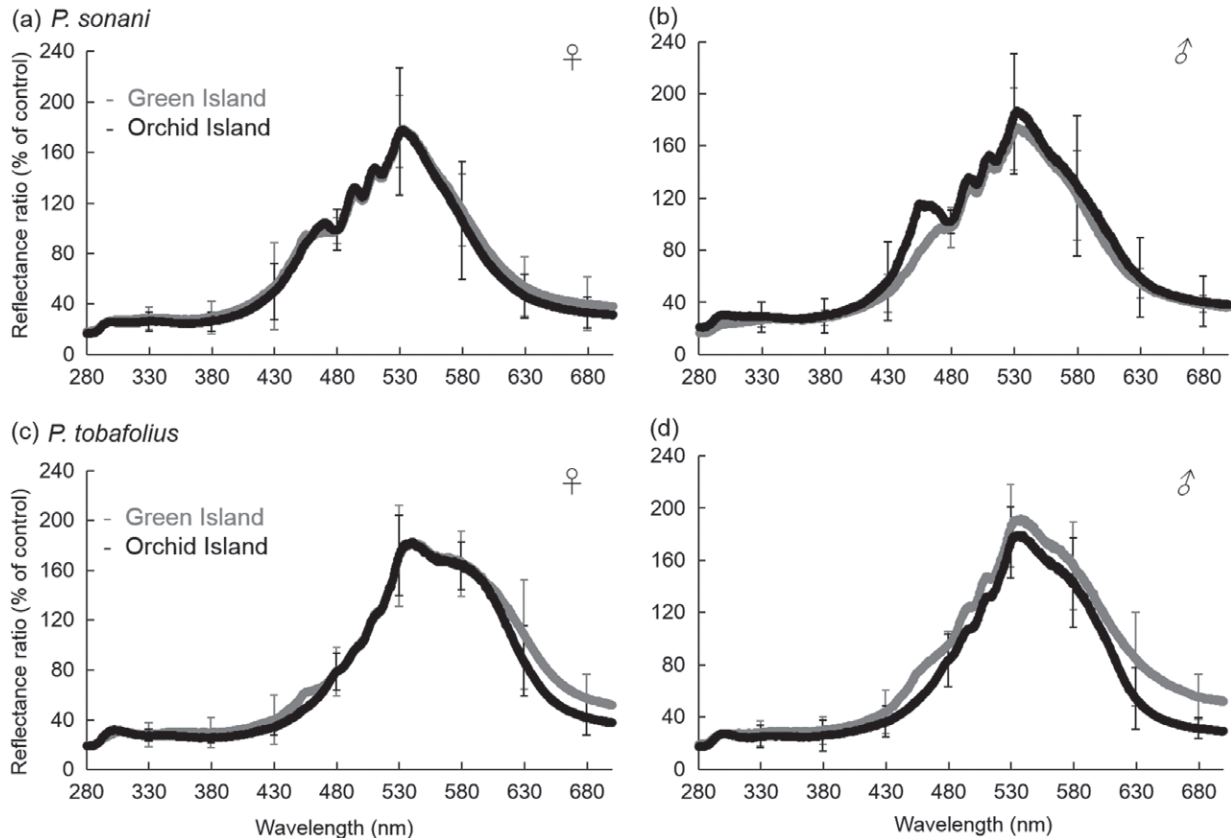


Fig. 3. Colour spectra of the cuticular scales of the island populations of *Pachyrhynchus sonani* (a, b) and *Pachyrhynchus tobafolius* (c, d).

Optics). We measured the reflectance spectra of individuals five times, and the mean values of colour parameters (hue, brightness and saturation) were calculated and used for the analyses. The hue was defined as the wavelength at the highest peak of the reflectance spectrum, and the brightness was defined as the reflection ratio of the wavelength at the highest peak of the spectrum. The colour saturation was defined as the total area below the reflectance curve that was between the visible spectrum of the diurnal lizard predators (440–625 nm), which generally have four spectrally distinct classes of colour vision, including ultraviolet-sensitive (UVS) (364–383 nm), short wavelength-sensitive (SWS) (440–467 nm), medium-wavelength sensitive (MWS) (483–501 nm) and long-wavelength-sensitive (LWS) (560–625 nm) visual pigments (Loew *et al.*, 2002; Yewers *et al.*, 2015). The UVS wavelength area was not used to calculate colour saturation because both *P. sonani* and *P. tobafolius* had low UV reflectance (Fig. 3, <40%). The significance of the spectral difference between island populations was tested using ANOVA in SPSS.

To characterize the fine-scale morphology of colour scales, the cuticular scales on the surface of colour stripes were coated with platinum-palladium (300 Å) using an ion coater (Model IB-2; Eiko, Taipei, Taiwan) and then observed through a scanning electron microscope (SEM) (SU1510; Hitachi, Tokyo, Japan). The number of scales and scale types in a pre-defined area

(450×337.5 μm²) [*P. sonani* ($n = 41$), stripe crossing the left elytra (Fig. 2a, square e); *P. tobafolius* ($n = 21$), the second dorsal spot of the left elytra (Fig. 2a, square f)] were recorded using SEM photographs at 400× magnification. The scale types were defined as follows: type I, the carving area is <two-thirds of the scale surface (Fig. 4a); type II, the carving area is >two-thirds of the scale surface (Fig. 4b); type III, the carving area is >two-thirds of the scale surface, and the scale has a major depression in a half-moon shape (Fig. 4c). The number of scales and the frequency of scale types were analysed using ANOVA and chi-squared statistics, respectively, in SPSS.

DNA extraction, sequencing and phylogenetic analyses

Genomic DNA was extracted from the legs of the weevils using a FavorPrep Tissue Genomic DNA Extraction Mini Kit (Favorgen Biotech Corp., Ping-Tung, Taiwan). The fragments of mitochondrial cytochrome c oxidase I (*cox1*, 700 bps), NADH dehydrogenase subunit 2 (*nd2*, 1000 bps), nuclear elongation factor 1α (*EF1α*, 800 bps) and internal transcribed spacer (*ITS*, 1700 bps) were amplified using the published [*cox1* (LCO-1490 and HCO-2198; Folmer *et al.*, 1994), *EF1α* (EF1-Bf and EF-Br; Hernández-Vera *et al.*, 2013) and *ITS* (ITS18Sr and ITS 28Sr; Weekers *et al.*, 2001)] and newly designed primers [*nd2*,

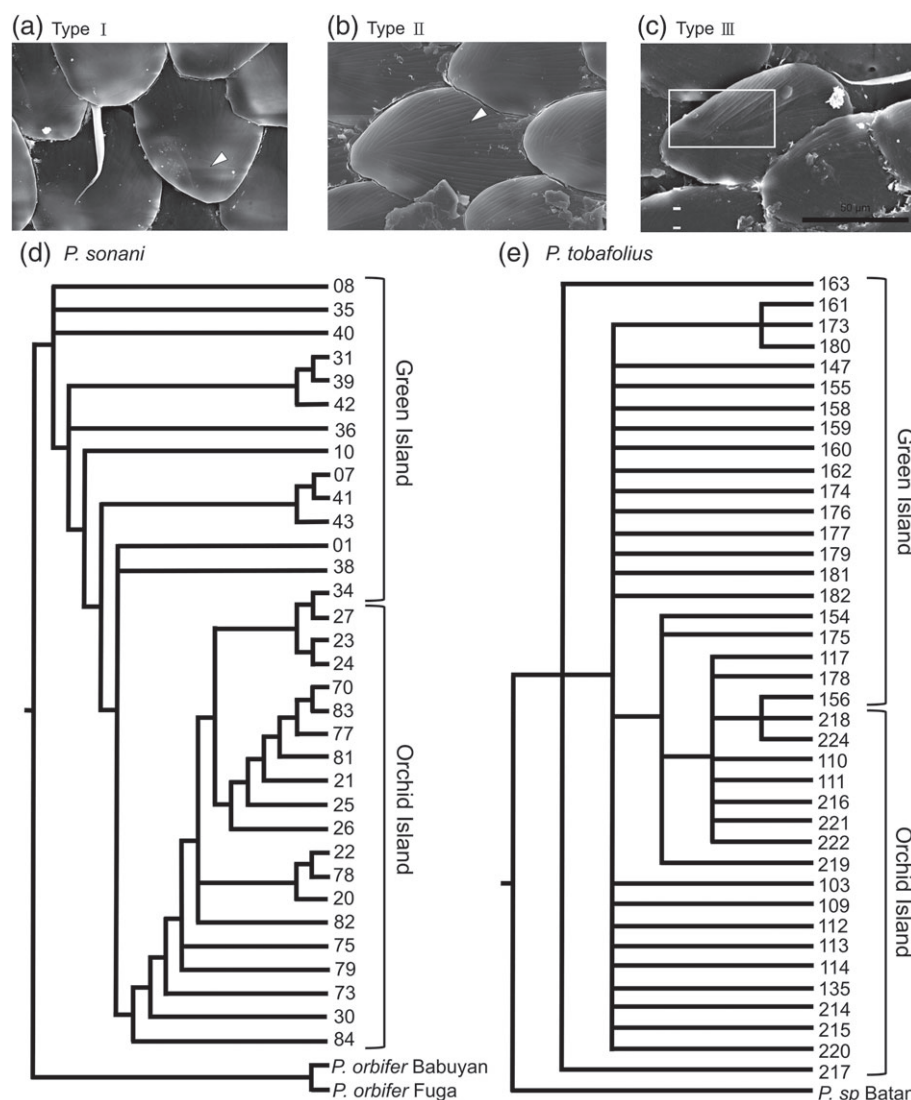


Fig. 4. Fine morphology of the cuticular scales of *Pachyrhynchus sonani*. (a) Type I, white arrow indicates carving area of less than two-thirds of scale surface. (b) Type II, white arrow indicates carving area of greater than two-thirds of scale surface. (c) Type III, white rectangle indicates a major depression in the shape of a half-moon. Maximum parsimony trees of *P. sonani* (d) and *P. tobaefolius* (e) based on 20 and four discrete colour traits (Appendix S5), respectively. All branches of these two parsimony trees had low bootstrapping values (<50%).

5'–GATTACTGCTTGAATAGGATTAG–3' (P–ND2–F) and 5'–CATAATGAAAATAGATTGTGTCATG–3' (P–ND2–R); H.Y. Tseng *et al.*, unpublished data]. The polymerase chain reaction (PCR) was carried out in a thermocycler (9700; Applied Biosystems, Foster City, CA, U.S.A.) with the following profile: (i) an initial denaturation at 94°C for 3 min; followed by (ii) 35 cycles of denaturation at 94°C for 1 min, annealing for 45 s at 50°C for *cox1*, 46°C for *nd2*, 62°C for *EF1α* and 56°C for *ITS*, extension at 72°C for 1 min; and (iii) a final extension step at 72°C for 10 min. The 25 μL PCR reaction contained 1–2 μL of genomic DNA, 17.5 μL of ddH₂O, 2.5 μL of Pro Taq 10× buffer, 2 μL of dNTP, 1 μL of forward primer, 1 μL of reverse primer, and 0.5 μL of ProTaq (PROTECH, Taipei, Taiwan). The PCR products were purified by treatment with shrimp

alkaline phosphatase/exonuclease I (USB Products, Affymetrix, Cleveland, OH, U.S.A.) and then subjected to sequencing in an ABI 3730XL DNA Analyzer (Applied Biosystems).

The DNA sequences were manually edited using SEQMAN in DNASTAR (LASERGENE, Swindell & Plasterer, 1997) and then aligned using CLUSTALW in MEGA v. 6.06 (Tamura *et al.*, 2013) (GenBank accession numbers in Appendix S2). For *ITS* alignment, the sequences were manually adjusted to minimize the gaps (indels were short, ≤3 nucleotides). *Pachyrhynchus orbifer* (Babuyan, Calayan, Camiguin, Dalupiri and Fuga Islands) and *P. infernalis* (Yaeyama Islands) were used as outgroups for the *P. sonani* phylogenetic analyses because of their close relationships (H.Y. Tseng *et al.*, unpublished data), and the *Pachyrhynchus* sp. of Batan Island, which is morphologically

similar to *P. tobafolius*, was used as an outgroup. Maximum parsimony (MP) analyses were conducted in PAUP* v. 4.0b10 (Swofford, 2002) using a parsimony ratchet algorithm implemented in PAUPRAT (Nixon, 1999; Sikes & Lewis, 2001) to search for the most parsimonious trees. Parsimony bootstrapping (PB) (Felsenstein, 1985) was conducted with heuristic searches of 1000 replications, and each replication contained 100 iterations of the tree-bisection-reconnection swapping algorithm. Maximum likelihood (ML) analyses were conducted using RAXML v. 8.2 (Stamatakis, 2006) under the GTRGAMMA model with the data partitioned by genes to accommodate the rate heterogeneity among sites, and the ML analyses generated 1000 distinct ML trees from 1000 randomly selected parsimony trees. Likelihood bootstrapping was conducted using 1000 iterations with randomly selected starting trees. The best-fit nucleotide substitution model from the Bayesian analyses was selected based on the Bayesian information criterion using JMODELTEST v. 2.1.7 (Darriba *et al.*, 2012): *P. sonani*, JC for nt1 of *cox1*, F81 for nt2 of *cox1*, TIM3 + I for nt3 of *cox1*, HKY for nt1 of *nd2*, HKY for nt2 of *nd2*, TrN for nt3 of *nd2*, JC for nt1 and nt2 of *EF1 α* , F81 for nt3 of *EF1 α* , TrN for nt1 of *ITS*, and HKY for nt2 and nt3 of *ITS*; *P. tobafolius*, TrNef for nt1, TIM3 for nt2, and HKY + I for nt3 of *cox1*. Bayesian analyses were conducted in MRBAYES v. 3.2 (Ronquist *et al.*, 2012) using the Markov chain Monte Carlo (MCMC) searches for 2×10^8 generations with a sampling frequency of every 10 000 generations and a burn-in of 2.5×10^7 generations. The burn-in value was determined by plotting the likelihood scores of the sampled trees against generation time. All trees sampled before reaching stability of the likelihood scores are discarded as burn-in. The convergence of the MCMC runs was confirmed using the effective sample size (ESS) of the model parameters (ESS mean for *P. sonani*: *cox1* = 9001, *nd2* = 9001, *EF1 α* = 8937.5, *ITS* = 8917.5, and combined = 9001; *P. tobafolius*: *cox1* = 8735). The Bayesian posterior probability was calculated from a 50% majority rule tree after discarding a burn-in of 25% of the trees. The coloration of the weevils was coded as 20 and four discrete characters for *P. sonani* and *P. tobafolius*, respectively (Appendix S3–S6), and the colour character matrices (Appendices S3, S4) were used for parsimony analyses in PAUP* with a PAUPRAT ratchet algorithm.

Library preparation, RAD sequencing and population genetic structure

The DNA samples were extracted using a Qiagen Blood and Tissue DNA Extraction Kit (Qiagen, Boston, MA, U.S.A.) from the thoracic muscles of the weevils and then suspended in TE buffer and stored at -20°C in the Genome Sequencing Core of the University of Kansas. They were then quantified using a Qubit dsDNA HS Assay Kit (Thermo Fisher Scientific Inc., Boston, MA, U.S.A.) and diluted into 5 ng/ μL in a total volume of 10 μL , which resulted in 50 ng of DNA for each sample for library preparation. We followed the multiplexed shotgun sequencing protocol (Andolfatto *et al.*, 2011) for library preparation. The genomic DNA samples were first digested using a *Nde*I (5'–CA[^]TATG–3') restriction enzyme, and the

individual barcodes and adaptors were then ligated to the digested genomic DNA samples. The individually barcoded RAD samples were pooled and precipitated overnight, and we then size-selected the pooled RAD samples from 350 to 450 bps and eluted the DNA fragments in the targeted range in a Pippin Prep System (Thermo Fisher Scientific Inc.). The eluted samples were separated for enrichment into four PCR reactions using FCR1 and FCR2 primers; the PCR products were pooled, purified and then single-ended sequenced in a HiSeq 2500 system (Illumina, San Diego, CA, U.S.A.). The sequencing reads were preliminarily screened in PROCESS RADTAGS (Illumina) for adaptor sequence contamination and then de-multiplexed based on the individual barcodes of 6 bp. We followed the standard STACKS pipeline for SNP-calling (Catchen *et al.*, 2013). The de-multiplexed reads from the individual genome were stacked in USTACKS, and CSTACKS was used to generate the SNP catalogue for all samples. SSTACKS was used to match the SNPs from the individual genome to the catalogue, and we proposed that the samples from the two islands were individual populations. We called SNPs using at least 10 \times in the sequencing coverage and allowed up to 50% missing data in an SNP and 30% missing data among populations. The SNP data were output into different data formats for analyses using POPULATIONS, and we used the Bayesian clustering method in STRUCTURE v. 2.3.4 (Falush *et al.*, 2003) to determine the level of the population admixture and identify the potential migrants and hybrids. The MCMC process was run for 2×10^6 generations with a burn-in of 5×10^5 generations. The estimated number of clusters (*K*) was set to range from 1 to 10 for all individuals to explore their optimal values, and the delta *K* statistic was calculated to determine the most appropriate number of genetic clusters in STRUCTURE HARVESTER web v. 0.6.94 (Earl & vonHoldt, 2012).

Integrated species delimitation

For *P. sonani* iBPP analyses, individuals were assigned to putative taxa based on island origin, clustering of phenotypic traits and a uniform rooted guide tree (Fig. 5b) ($n = 14$ males and five females from Green Island, and 11 males and 6 females from Orchid Island). The character matrix included: (i) biogeographical (location of island); (ii) molecular (*cox1*, *nd2*, *EF1 α* and *ITS*); and (iii) morphological traits [the first PC scores for the dorsal and lateral body shape, the first PC scores for coloration (hue, brightness and saturation), the number of scales, the frequency of scale types, discrete colour traits (traits 5, 6, 9, 10, 11, 12, 13, 14, 18 and 19 in Appendices S3, S5) and the first PC scores for the male and female genitalia]. We specified four combinations of the prior distribution for the ancestral population size (θ) and the root age of the tree (τ): (i) $\theta = G$ (1, 10) and $\tau = G$ (1, 10), assuming large population sizes and a deep divergence time; (ii) $\theta = G$ (1, 10) and $\tau = G$ (2, 2000), representing large population sizes and a shallow divergence time; (iii) $\theta = G$ (2, 2000) and $\tau = G$ (1, 10), indicating small population sizes and a deep divergence time; and (iv) $\theta = G$ (2, 2000) and $\tau = G$ (2, 2000), signifying small population sizes

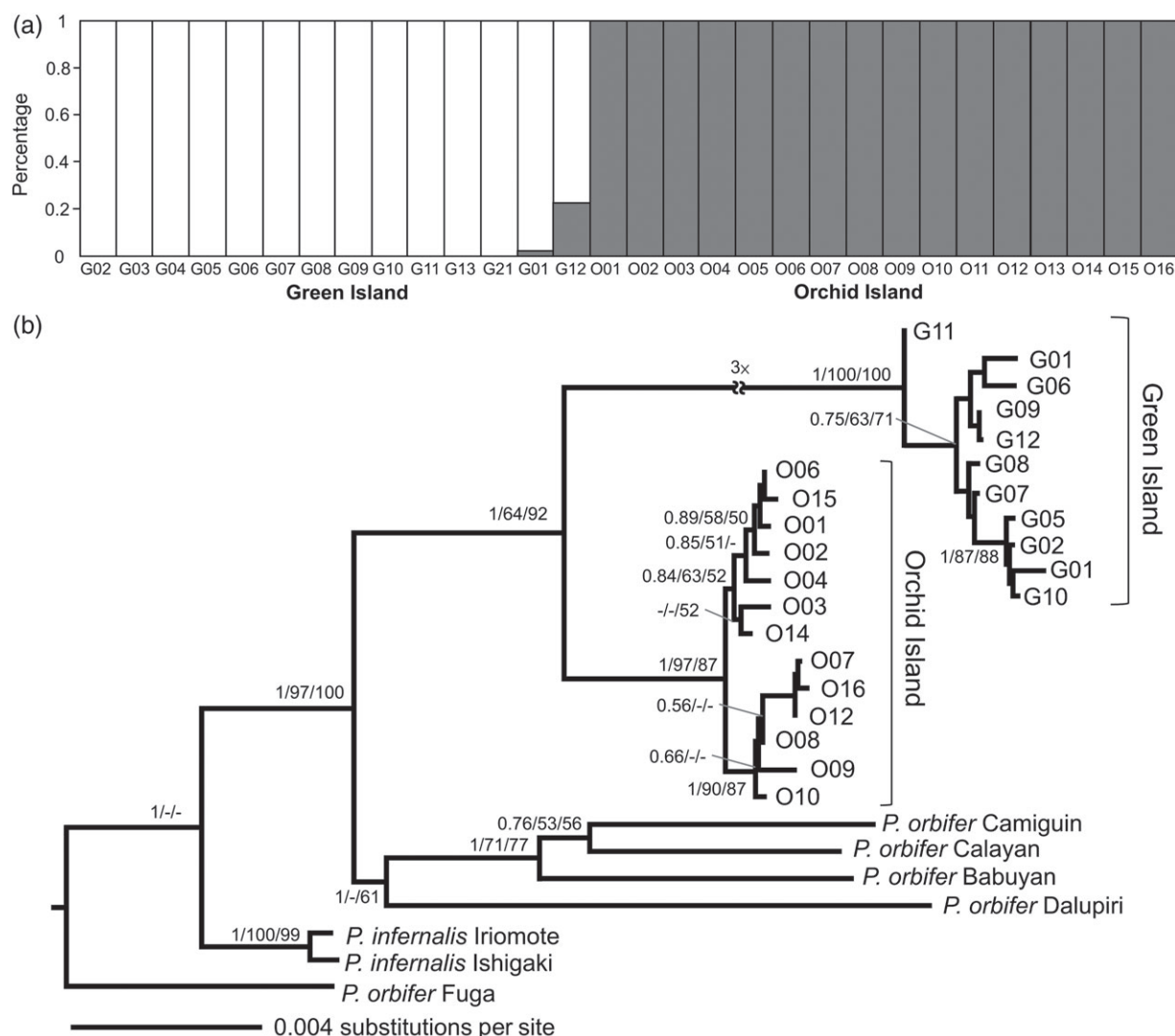


Fig. 5. (a) STRUCTURE genetic clustering analyses for *Pachyrhynchus sonani*. The optimal genetic clustering model was $K=2$. (b) Phylogeny of *Pachyrhynchus sonani* reconstructed from Bayesian phylogenetic analyses based on four genes (*cox1*, *nd2*, *EF1α* and *ITS*). Numbers near the nodes are the branch support values of the Bayesian posterior probability/parsimony bootstrap/likelihood bootstrap. Nodes without numbers have support values of <50%.

and a shallow divergence time (Zhang *et al.*, 2011). The analysis was run for 5×10^5 generations using the proposal algorithm 1 of the rjMCMC (reversible-jump MCMC) species delimitation and fine-tuning parameters (Yang & Rannala, 2010) adjusted for an acceptance rate ~30% with a sampling frequency of 1000 generations and a burn-in of one-quarter of the iterations (1.25×10^5 generations). The parameters of the locus-specific rates of evolution were fine-tuned using an auto option.

Results

Host plant range

We obtained a total of 102 *P. sonani* (Green Island = 63, Orchid Island = 39) and 110 *P. tobaefolius* (Green Island = 74,

Orchid Island = 36) specimens (Appendix S1). The host plants of *P. sonani* from Orchid Island were mainly the sea poison tree, *Barringtonia asiatica* (Lecythidaceae) (93.75%), but weevils were occasionally found on beef wood, *Casuarina equisetifolia* (Casuarinaceae) (3.13%) and Indian almond, *Terminalia catappa* (Combretaceae) (3.13%). In contrast, the host plants of *P. sonani* from Green Island were largely Ceylon ardisia, *Ardisia elliptica* (Primulaceae) (50%) and beef wood (48%), and only occasionally litsea, *Litsea acutivens* (Lauraceae) (2%), with no records on the sea poison tree that also occurs on that island. The *P. tobaefolius* host plants from Green Island were all mulberry, *Pipturus arborescens* (Urticaceae) (100%), while those from Orchid Island were largely mulberry (82.86%) and, less frequently, copperleaf, *Acalypha caturus* (Euphorbiaceae) (17.14%). The frequencies of the utilized host plant species

were significantly different between the island populations of *P. sonani* ($\chi^2 = 77.966$, $P < 0.001$) and *P. tobafolius* ($\chi^2 = 8.693$, $P = 0.003$). Our host plant data were based on an association of feeding and presence of adult weevils on a plant species. Because the adults are mobile and may be on the plant in transit, further studies using an association of larval feeding or molecular characterization of gut content and faeces of the adult are necessary to confirm the host plant range.

Shape and size of the body and genitalia

The MANCOVA of 12 body shape measurements revealed that both *P. sonani* and *P. tobafolius* were sexually dimorphic ($P < 0.001$) and indicated that the island populations of both species were significantly different in their body shapes (*P. sonani*, $P = 0.004$; *P. tobafolius*, $P = 0.013$). Landmark-based morphometric analyses also indicated sexual dimorphism in both species (Appendix S7) and that the lateral body shapes of the island populations of female *P. sonani* were significantly different (Goodall's $F = 2.27$, $P = 0.004$) (Fig. 6c), while their dorsal body shapes were similar (Goodall's $F = 0.88$, $P = 0.604$) (Fig. 6a). The female *P. sonani* from Green Island had a curvier body than those of Orchid Island (Fig. 6d), and the island populations of male *P. sonani* differed in both their dorsal and lateral body shapes (dorsal, Goodall's $F = 1.68$, $P = 0.040$; lateral, Goodall's $F = 1.70$, $P = 0.044$) (Fig. 6e, g). The male *P. sonani* of Green Island had a longer, flatter rostrum and a shorter abdomen than did those of Orchid Island (Fig. 6f). The island populations of *P. tobafolius* differed in their dorsal body shapes (Fig. 6i, m; male, Goodall's $F = 10.88$, $P < 0.001$; female, Goodall's $F = 4.66$, $P < 0.001$). The female *P. tobafolius* of Green Island had a shorter rostrum and a wider, longer and flatter abdomen than those of Orchid Island (Fig. 6j), whereas the male *P. tobafolius* of Green Island had a shorter rostrum and head, an anteriorly extended thorax, and a wider abdomen than did those of Orchid Island (Fig. 6n).

The island populations of *P. sonani* had significantly different aedeagus size (measurements: Green Island 2.52 ± 0.02 mm; Orchid Island 2.65 ± 0.02 mm, $t = -2.686$, $P = 0.012$; centroid size: Green Island 27.72 ± 1.41 ; Orchid Island 28.97 ± 1.06 ; $t = -3.050$, $P = 0.004$), whereas the island populations of *P. tobafolius* were similar in their aedeagus size (measurements: Green Island, 2.24 ± 0.02 mm; Orchid Island, 2.26 ± 0.01 mm; $t = -0.508$, $P = 0.616$; centroid size: Green Island, 26.59 ± 1.66 ; Orchid Island, 27.04 ± 2.12 ; $t = -0.871$, $P = 0.392$). The sizes of the female genitalia of the island populations were similar for both *P. sonani* (measurements: Green Island, 0.715 ± 0.003 mm; Orchid Island, 0.721 ± 0.002 mm; $t = -0.192$, $P = 0.85$; centroid size: Green Island, 8.67 ± 0.21 ; Orchid Island, 9.07 ± 0.33 ; $t = -1.329$, $P = 0.213$) and *P. tobafolius* (measurements: Green Island, 0.958 ± 0.008 mm; Orchid Island, 0.998 ± 0.012 mm; $t = -0.632$, $P = 0.55$; centroid size: Green Island, 10.01 ± 0.29 ; Orchid Island, 10.00 ± 0.46 ; $t = 0.001$, $P = 0.999$). For *P. sonani*, the aedeagus shape of the Green Island population showed

significantly more curvature and were thinner than those of Orchid Island (Goodall's $F = 1.95$, $P = 0.008$; without the outlier no. 19, Goodall's $F = 2.07$, $P = 0.004$) (Fig. 2e, f), whereas the island populations of *P. tobafolius* were similar in their aedeagus shape (Goodall's $F = 0.83$, $P = 0.679$) (Fig. 2g). In contrast, the shape of the female genitalia of the island populations were similar for both *P. sonani* (Goodall's $F = 1.36$, $P = 0.245$) and *P. tobafolius* (Goodall's $F = 0.53$, $P = 0.784$) (Fig. 2h, i).

Colour pattern and scale traits

The reconstructed parsimony tree from 20 discrete colour characters (19 informative characters) (Fig. 4d) suggested that the Green Island population of *P. sonani* was polyphyletic, while the Orchid Island population consisted of a monophyletic lineage, except for one Green Island individual (no. 34, female) nested within the Orchid Island clade. This individual has a typical colouration of the Orchid Island population (two elongate posterior-lateral colour stripes on the elytra). In contrast, the *P. tobafolius* parsimony tree (four informative characters) resulted in no clear grouping according to island origins (Fig. 4e). All branches of these two parsimony trees had low bootstrapping values ($< 50\%$), which was probably due to the small number of colour characters or character incongruence (consistency index, CI: *P. sonani*, 0.318; *P. tobafolius*, 0.571). There were no significant differences between the colour spectra of the cuticular scales of the island populations of both *P. sonani* and *P. tobafolius* (Fig. 3), but the male and female *P. tobafolius* had significantly different hues (male, 537.04 ± 7.96 nm; female, 546.53 ± 15.55 nm; $P = 0.036$) and saturation levels (male, $74.17 \pm 3.47\%$; female, $71.09 \pm 4.29\%$; $P = 0.043$). The cuticular scale density of *P. sonani* was higher in the Green Island population than in that of Orchid Island (Green Island, $56.20 \pm 9.19/450 \times 337.5 \mu\text{m}^2$; Orchid Island, $47.10 \pm 9.07/450 \times 337.5 \mu\text{m}^2$; $P = 0.003$), and the type III scales were only found in the *P. sonani* females from both islands. The frequencies of the scale types in the male *P. sonani* were significantly different between the island populations, with the Green Island population only having type II scales (Green Island: type II, 100%, $n = 11$; Orchid Island: type I, 36.36%, $n = 4$; type II, 63.64%, $n = 7$; $\chi^2 = 4.889$, $P = 0.027$). The frequencies of the scale types were similar between the island populations of female *P. sonani* (Green Island: type I, 11.11%, $n = 1$; type II, 66.67%, $n = 6$; type III, 22.22%, $n = 2$; Orchid Island: type I, 40%, $n = 4$; type II, 50%, $n = 5$; type III, 10%, $n = 1$; $\chi^2 = 2.178$, $P = 0.337$). The frequencies of the scale types were significantly different between the island populations of female *P. tobafolius* (Green Island: type I, 60%, $n = 3$; type II, 40%, $n = 2$; Orchid Island: type II, 100%, $n = 5$; $\chi^2 = 4.286$, $P = 0.038$) but were not significantly different between the male *P. tobafolius* populations (Green Island: type I, 40%, $n = 2$; type II, 60%, $n = 3$; Orchid Island: type II, 100%, $n = 6$; $\chi^2 = 2.933$, $P = 0.087$).

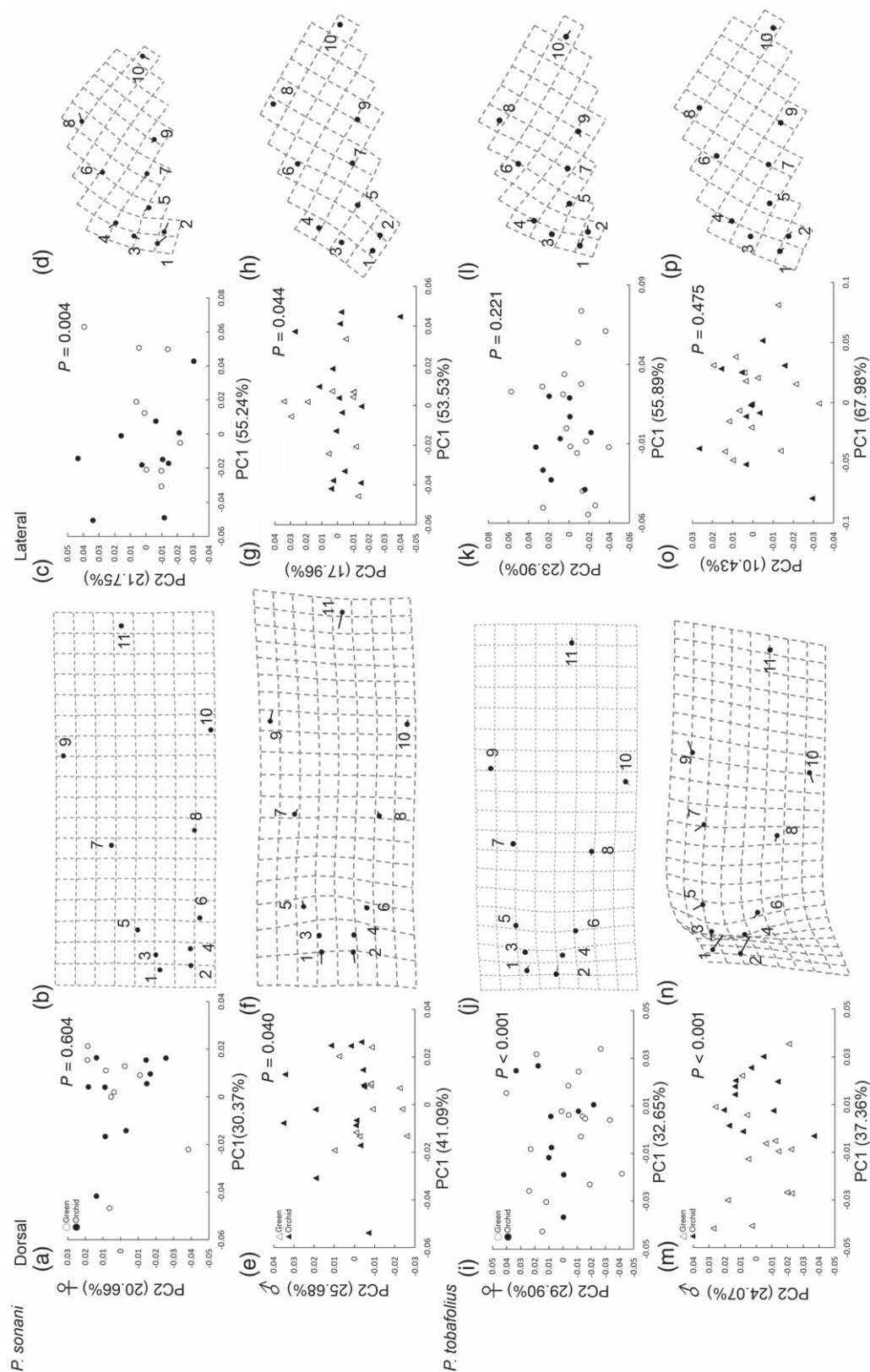


Fig. 6. Landmark-based morphometric analyses of the body shapes of the island populations of *Pachyrhynchus sonani* (a–h) and *Pachyrhynchus tobafolius* (i–p). (a, c) Females of *P. sonani*: (a) dorsal view, (c) lateral view. (e, g) Males of *P. sonani*: (e) dorsal view, (g) lateral view. (i, k) Females of *P. tobafolius*: (i) dorsal view, (k) lateral view. (m, o) Males of *P. tobafolius*: (m) dorsal view, (o) lateral view. Body shape deformation grid from the Orchid to Green Island populations (5×) – (b, d) females of *P. sonani*: (b) dorsal view, (d) lateral view; (f, h) males of *P. sonani*: (f) dorsal view, (h) lateral view; (j, l) females of *P. tobafolius*: (j) dorsal view, (l) lateral view; (n, p) males of *P. tobafolius*: (n) dorsal view, (p) lateral view.

Population genetic structure and molecular phylogeny

Restriction site-associated DNA sequencing resulted in 2004 and 303 SNPs for *P. sonani* and *P. tobafolius*, respectively. The smaller number of SNPs in *P. tobafolius* than in *P. sonani* suggested overall lower genomic divergence between and within populations of *P. tobafolius*. Bayesian clustering analyses of the SNPs demonstrated that the *P. sonani* individuals were best grouped into two genetic clusters of the same island of origin (Fig. 5a) ($K = 2$, $\ln L = -8541.94 \pm 1.44$; $\Delta K = 2$ had the highest peak; Appendix S8a, c), whereas the members of *P. tobafolius* could not be unambiguously assigned into any number of genetic clusters (models with $K = 1-10$ are equally probable; Appendix S8b, d), suggesting that they belong to the same gene pool or a large number of loci may be required to detect differentiation. The four-gene dataset contained a total of 4050 bp (*cox1* 675, *nd2* 983, *EF1a* 810 and *ITS* 1582 bps). The *cox1* and *nd2* gene trees (Appendix S9a, b) indicated that each of the *P. sonani* populations form a monophyletic lineage but sister to *P. orbifer* (*cox1*), and *P. infernalis* and *P. orbifer* (*nd2*). The *EF1a* and *ITS* gene trees (Appendix S9c, d) showed a paraphyletic *P. sonani* from Orchid Island with respect to a monophyletic *P. sonani* of Green Island. The topological incongruence between mitochondrial and nuclear gene trees might result from lineage sorting, sex-biased dispersal or hybridization of ancestral lineages. The *cox1* and *nd2* gene trees have relatively long branches leading to the Green Island population, whereas the *EF1a* and *ITS* gene trees have more even tree branches for the same population (Appendix S9). The long tree branch observed for the Green Island population is probably due to balancing selection, which preserves these mitochondrial haplotypes for longer than expected under genetic drift (ancestral population subdivision would be expected if all gene trees had long branches for Green Island population). The combined phylogeny of the four genes established strong support for two monophyletic and sister *P. sonani* of Green Island (1/100/100, BPP/PB/LB) and Orchid Island (1/97/87, BPP/PB/LB) (Fig. 5b) (TreeBASE accession no. 21075). There were two divergent lineages within the Orchid Island clade. In contrast, the *P. tobafolius cox1* phylogeny (677 bps) had short branches, lacked resolution and revealed no phylogenetic clustering of the island lineages (Appendix S10). One individual (G03) from Green Island had a long branch, which may represent a unique ancestral haplotype, a descent of recent migrant or a misplaced taxon due to long-branch attraction in phylogenetic analyses.

Integrated species delimitation

Bayesian species delimitation of the integrated dataset suggested the presence of two species of *P. sonani* from Green Island and Orchid Island, which was supported by a divergent node with a posterior probability of 1.0 (ESS of all the parameters in the MCMC runs $>11\,800$) under various prior population demography and species divergence time settings (large versus small ancestral population sizes, θ , and deep versus shallow divergence times, τ) (Appendices S11, S12).

Taxonomy

***Pachyrhynchus jitanasaius* sp.n. Chen & Lin (Fig. 7)**

<http://zoobank.org/urn:lsid:zoobank.org:act:3246D9EB-425D-45AC-B68F-9EA067ABA5B2>

Diagnosis. *Pachyrhynchus jitanasaius* sp.n. is morphologically very similar to *Pachyrhynchus sonani* Kôno. *Pachyrhynchus sonani* was originally described from specimens collected on Orchid Island (Kotosho) using the following combination of colour characteristics (Kôno, 1930): head with a lateral scale band extending from the rostrum to behind the eyes, prothorax with a T-shaped scale band, elytra with two scale bands extending from the anterior to the rear end. *Pachyrhynchus jitanasaius* sp.n. can be identified by the absence of the posterior-lateral elytrous stripes or with small spherical spots but rarely with two stripes (Fig. 7a, c, L3 and R3), whereas *P. sonani* usually exhibits one or two elongate stripes at the same position. In addition, the aedeagus of *P. jitanasaius* sp.n. has greater curvature and is thinner than that of *P. sonani* (Fig. 7e, f).

Description. Measurements (mean \pm SE) (mm). Males ($n = 12$): RW, 1.36 ± 0.12 ; HW, 2.47 ± 0.16 ; TW, 3.84 ± 0.25 ; AW, 5.34 ± 0.30 ; RL, 1.78 ± 0.12 ; HL, 3.16 ± 0.21 ; TL, 3.67 ± 0.26 ; AL, 7.81 ± 0.46 ; RH, 1.38 ± 0.13 ; HH, 2.47 ± 0.15 ; TH, 3.21 ± 0.25 ; AH, 4.53 ± 0.12 ; AEL ($n = 16$), 2.54 ± 0.01 . Females ($n = 9$): RW, 1.39 ± 0.08 ; HW, 2.46 ± 0.09 ; TW, 3.76 ± 0.20 ; AW, 5.87 ± 0.29 ; RL, 1.75 ± 0.11 ; HL, 3.20 ± 0.26 ; TL, 3.45 ± 0.16 ; AL, 8.17 ± 0.55 ; RH, 1.40 ± 0.14 ; HH, 2.46 ± 0.16 ; TH, 3.16 ± 0.24 ; AH, 4.83 ± 0.30 ; SW ($n = 7$), 0.715 ± 0.003 .

Body dark black with green, shiny blue and green stripes and spots. Rostrum with short pubescence and sporadic scales near mouthparts. Head with sparsely short pubescence behind eyes. Lateral head with a scale band extending from rostrum to behind eyes. Triangle-like scale spot between fronts of eyes and vertex. Dorsal prothorax with a T-shaped scale band at centre (Fig. 7a). Scales cover entire prosternum (Fig. 7b). Elytral scale stripes consist of a horizontal scale band at the centre, and two circular scale bands at anterior and posterior halves of the elytra, with connection to the horizontal scale band at lateral ends, but not at the centre (Fig. 7a, c). Area of L1, R1, L3 and R3 spotless (Fig. 7c, d). Abdominal ventrite I with two horizontal scale bands not connected to each other (Fig. 7b). Ventrite II with a connected horizontal scale band. Ventrites III, IV and V without scale bands. Legs black, coxa, trochanter and tibia black without scales but femur with two broken scale bands. Femur and tibia of approximately equal length. Tibia with short strong hairs. Tarsus black and covered with pubescence on segments I, II, III, IV and pad.

Head bends down with short rostrum and weakly bulging eyes. Antennae with stout and slightly longer scape. Pedicel and flagella I, II, III, IV and V of similar size with short, thin pubescence. Flagellum VI gradually larger with short sporadic pubescence. Flagellum VII club and covered with short pubescence. Rostrum longer than wide (RW/RL: male, 0.76;

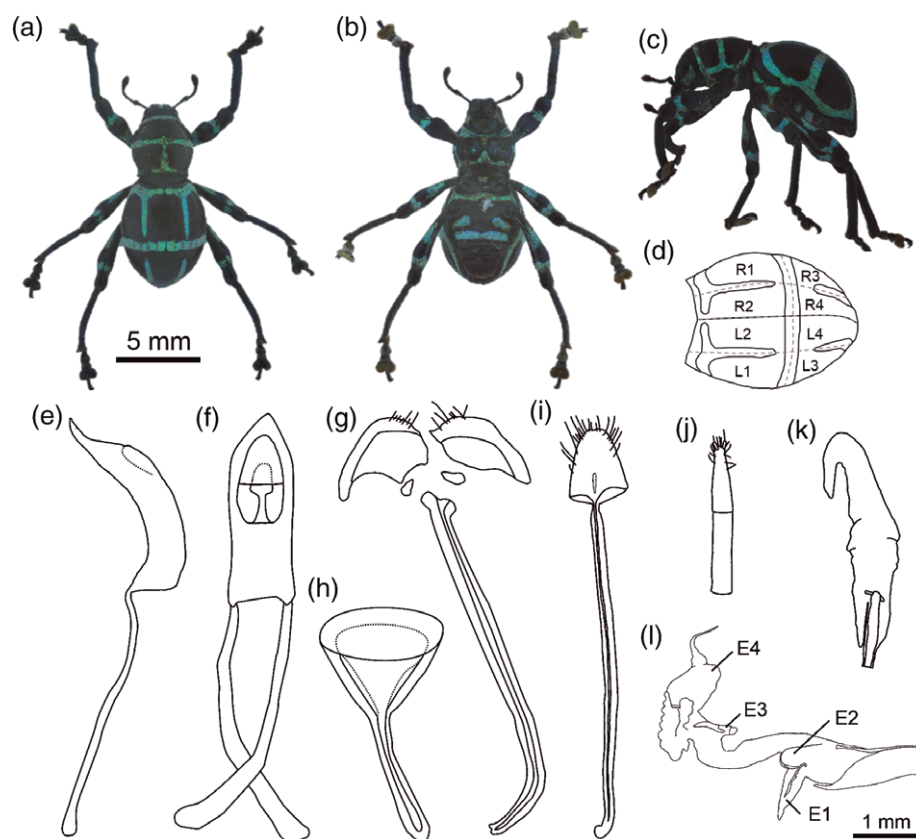


Fig. 7. Holotype of *Pachyrhynchus jitanasaius* sp.n.: (a) dorsal view, (b) ventral view, (c) lateral view, (d) area of the dorsal elytra. Male genitalia: aedeagus in dorsal view (e) and lateral view (f); (g) sternite IX in dorsal view; (h) tegmen in dorsal view. Female genitalia: (i) sternite VIII in ventral view; (j) ovipositor apex in dorsal view; (k) spermatheca. (l) Male endophallus in lateral view (E1, middle leaf; E2, globular leaf; E3, obreniform sclerite; E4, apical sclerite). [Colour figure can be viewed at wileyonlinelibrary.com].

female, 0.79), minutely punctured, weakly bulging anteriorly and gradually declined to apex. Subspherical prothorax minutely punctured, about as long as wide (TW/TL: male, 1.05; female, 1.08). Dorsal prothorax shallowly convex. Elytra subobovate and convex with seven weak punctural striae. Length of elytra twice as long as the prothorax (AL/TL: male, 2.13; female, 2.37). Width of elytra 1.5 times longer than prothorax (AW/TW: male, 1.39; female, 1.56). Abdomen broadest at one-third of ventrites.

Male (Fig. 7e–h, l) and female genitalia (Fig. 7i–k) as illustrated. Aedeagal body (Fig. 7e, f) curved near base; sides subparallel to apical one-fourth and tapering toward apex with aedeagal apodemes slender and slightly longer than aedeagal body. Spiculum gastrale (Fig. 7g) longer than aedeagal body and curved rightward. Tegmen (Fig. 7h) short and stout. Endophallus (Fig. 7l) with trifid near sub-base one-third. Middle leaf (E1) sharp, two globular leaves (E2) connected with each other, obreniform sclerite (E3) midway, a sclerite along apical one-third inflate (E4) with folds and connected with flagellum. In female genitalia, sternite VIII (Fig. 7i) spade-shaped with short hairs at apical margin and a slender stem at base. Stem three times longer than main part of sternite VIII. Apex of ovipositor (Fig. 7j) slender and gradually sharp in apical

one-half with two small sclerites and short hairs. Spermatheca (Fig. 7k) saccular without sclerite.

Key to *Pachyrhynchus* species of Green and Orchid Islands

- 1a. Prothorax has four dorsal circular colour spots *P. tobafolius*
- 1b. Prothorax has three dorsal circular or stripe colour spots ... 2
- 2a. Prothorax has three dorsal circular colour spots ... 3
- 2b. Prothorax has dorsal colour stripes ... 4
- 3a. Head vertex has one dorsal colour spot *P. sarcitis kotoensis*
- 3b. Head vertex dorsal colour spot absent ... *P. insularis*
- 4a. Prothorax dorsal crossing colour stripe absent. *P. yamianus*
- 4b. Prothorax has a dorsal T-shaped colour stripe at centre ... 5
- 5a. One or two extensions from the colour stripe at L1 and R1 of elytra (Figs 1d, e, 7d) ... *P. sonani*
- 5b. No extension of the colour stripe at L1 and R1 of the elytra (Figs 1e, 7c, d) ... 6
- 6a. Linear colour stripe connected to posterior colour stripe at L3 or R3 of the elytra (Figs 1d, e, 7d) ... *P. sonani*
- 6b. No or round colour spot at L3 and R3 of the elytra (Figs 1e, 7c, d) ... *P. jitanasaius* sp.n.

Type material. Holotype male (specimen code, Ps365) '[Taiwan]/Taitung County, Green Island/VII. 2014, collector' (typed

on a white card), 'YEN-TING CHEN/COLLECTION' (typed on a white card), '[Holotype] Male/*Pachyrhynchus jitanasaius*/Chen, 2016/Det. Chen *et al.*, 2016' (typed on a red card). Paratypes (3 exs.) (specimen code, Ps331, Ps315 & Ps285) '[Taiwan]/Taitung County, Green Island/VII. 2014, collector' (typed on a white card), 'YEN-TING CHEN / COLLECTION' (typed on a white card), '[Paratypes]/*Pachyrhynchus jitanasaius* / Chen, 2016/Det. Chen *et al.*, 2016' (typed on a specimen label). The holotype and paratypes were deposited in National Museum of Natural Science (NMNS), Taichung, Taiwan.

Distribution. TAIWAN: Green Island (Green Island Township, Taitung County).

Etymology. The new species is named after the type location, do Jintanasai, which is the name of Green Island in the aboriginal language of the Tao (Yami) people.

Discussion

The majority of morphological characters reveal overlapping but statistically significant difference between the island populations of *P. sonani* (Table 1), while the two molecular datasets indicate two separate lineages. Integrated species delimitation of combining morphological, molecular and ecological characters further strengthens the support for recognizing two distinct evolutionary lineages of *P. sonani*, each from Green Island and Orchid Island. In addition, diagnostic morphological (the posterior-lateral colour stripe of the elytra) and molecular (such as fixed, unique mitochondrial haplotypes) characters are identified and useful for distinguishing the different island populations of *P. sonani* in both field and laboratory settings. The identification of cryptic species relies on multiple characters (Barley *et al.*, 2013; Rato *et al.*, 2016), so integrated species delimitation based on multiple character types can provide a more quantitative and objective assessment of species diversity. For example, the species number of red-bellied snake species (genus *Storeria*) was reduced from eight to four when five morphological traits were added to a molecular dataset of genome-wide loci (Pyron *et al.*, 2016), and a recent example of integrated species delimitation in Hercules beetles (genus *Dynastes*) by combining molecular and morphological traits suggested ten species instead of one (Huang & Knowles, 2016). In contrast to *P. sonani*, most character sets indicate that the island populations of *P. tobafolius* show no detectable differentiation, which suggests that they belong to one species (Table 1) and is in agreement with earlier taxonomic assessments (Kano, 1929; Starr & Wang, 1992). The qualitative and quantitative evidence from our study provides a basis for a revision of the current taxonomy of *Pachyrhynchus* species in Taiwan. The endangered *P. sonani* is composed of two cryptic species, and the one from Green Island is described here as a new species, *P. jitanasaius* sp.n. Chen & Lin. In contrast, the two island populations of *P. tobafolius* should continue to be treated as one species. Based on our findings, we urgently recommend that the Wildlife Conservation Act of Taiwan revise the

species status of *P. sonani* and protect these two independently evolved island lineages. They have restricted distributions, limited gene flow and host preference, which make each more prone to extinction due to habitat loss.

Our results demonstrated that the molecular and phenotypical traits of *Pachyrhynchus* weevils differ in their level of divergence. Between island populations of *P. sonani*, molecular characters including nucleotide sequences and genome-wide SNPs showed a fixed and higher level of divergence, respectively, as compared with the morphological characters, except for one discrete colour character that revealed nonoverlapping differentiation. The biological processes underlying this pattern are not clear but might include the level of natural selection, the developmental and phylogenetic constraints on the traits, the extent of hybridization, and the direction and strength of gene flow between populations. An intriguing finding of this study was that, between island populations of *P. sonani*, almost all the male morphological traits diverged more than those of females, but no evidence has yet been found to suggest sexual selection for male traits in the divergence of *Pachyrhynchus* weevil species. All the male traits consistently distinguished the island populations of *P. sonani* as two separate species, while the female traits showed no significant divergence between the island populations (Table 1). Earlier taxonomic studies often regarded colour traits as highly polymorphic and unstable, thus making them unacceptable as diagnostic characters (e.g. *P. orbifer* complex; Schultze, 1923). However, our results suggest that the discrete colour traits of *P. sonani* are as useful as the traditionally applied male and female genital traits for species delimitation (Schultze, 1923; Yoshitake, 2012), so they can thus provide another source of informative characters for taxonomic and phylogenetic studies of *Pachyrhynchus* weevils. Although our study did not find fixed, diagnostic scale types between the island populations of *P. sonani*, the less frequently used fine structure of the cuticular scales, as observed through SEM (e.g. Erbey & Candan, 2014), can provide useful characters in the systematics of weevils, which as a group contains more species than any other major insect taxon (Oberprieler *et al.*, 2007). Other informative, even finer-resolution characters for discriminating *Pachyrhynchus* species may come from the use of three-dimensional photonic polycrystals (Welch *et al.*, 2007; McNamara *et al.*, 2013).

In sexually reproducing organisms, species are usually considered to be the central units of taxonomic characterization of global biodiversity (Wheeler *et al.*, 2012). The extent of morphological divergence between island populations of *P. sonani* indicates that they are consistently distinguishable morphological or phenetic species (Sokal, 1973), and the genetic clustering of *P. sonani* also establishes that its island populations consist of two valid evolutionary species with independent historical tendencies (Wiley, 1978). Based on our best phylogenetic estimation, the two *P. sonani* lineages from Green Island and Orchid Island are both monophyletic with respect to the outgroup taxa (Fig. 5b). According to an assumption of the exclusive monophyly of common ancestry, which is one of the many operational criteria of the phylogenetic species concept (de Queiroz & Donoghue, 1988; de Queiroz, 2007), these two

Table 1. Summary of *Pachyrhynchus sonani* and *Pachyrhynchus tobafolius* species delimitation based on multiple characters.

			<i>P. sonani</i>		<i>P. tobafolius</i>	
Characters			One species	Two species	One species	Two species
Molecular	RAD sequencing DNA sequences	SNPs		*	*	
		Four genes		*	* ^a	
Morphological	Body shape	Measurement		*♀, ♂		*♀, ♂
		GM (dorsal)	*♀	*♂		*♀, ♂
		GM (lateral)		*♀, ♂	*♀, ♂	
		Discrete characters		*	*	
	Coloration	Colour spectrum	*♀, ♂		*♀, ♂	
		Number of scales	*♀	*♂	*♀, ♂	
		Type of scales	*♀	*♂	*♂	*♀
		Measurement	*♀	*♂	*♀, ♂	
	Genitalia	Centroid size	*♀	*♂	*♀, ♂	
		GM	*♀	*♂	*♀, ♂	
	Host plant	Host plant range		*		*
		Integrated		*	NA	NA

^a*cox1* gene only.

GM, geometric morphometrics; RAD, restriction site-associated DNA; SNP, single nucleotide polymorphism. Asterisks indicate the presence (two species) and absence (one species) of a statistically significant difference between the Green Island and Orchid Island populations.

P. sonani lineages can be regarded as separate phylogenetic species. The *P. sonani* phylogeny has a relatively long branch separating the Green Island and Orchid Island lineages, suggesting that a substantial amount of mutation has accumulated over a certain period of time since their divergence, implying the extensive temporal separation of the two island species (~0.23 Ma, 95% CI: 0.08–0.46 Ma; H.Y. Tseng *et al.*, unpublished data). Nevertheless, to fully understand ‘the reality of species’ (*sensu* Coyne & Orr, 2004) and test the speciation process and biological species status (Mayr, 1995) of *P. sonani*, future experimental studies are needed to examine the level of reproductive isolation barriers and potential gene flow between the island populations.

Oceanic islands are powerhouses for generating endemic diversity, largely due to effects of geographical isolation, small population sizes and local adaptation. Situated on the northern boundary of the Kano's Line (‘New-Wallace Line’; Kano, 1941), Green Island and Orchid Island of the Taiwan-Luzon Archipelago are well known for their remarkable endemism (e.g. Kano, 1929; Yoshida *et al.*, 2000; Yen *et al.*, 2003; Hsu & Huang, 2008; Lee & Staines, 2010) and faunal and floral affinities with the Philippines (Kano, 1933, 1941; Li, 1953; Chang, 1986), although the two islands are geographically closer to Taiwan. However, to our knowledge, no previous study has attempted to examine closely the species boundary of the endemic organisms occurring on these two neighbouring islands using multiple character types. Our study of cryptic species in *P. sonani* represents the first empirical evidence indicating that the inter-island, allopatric speciation of the endemic organisms inhabiting Green and Orchid Islands may be more common than previously thought, but it has been concealed by morphologically or ecologically similar species. Therefore, our study emphasizes that the cryptic diversity of the endemic taxa of these two small oceanic islands may still be largely underestimated. For example, morphologically similar populations of a species of scarab beetle, *Anomala expansa*

(Rutelinae), has been found on Green Island and Orchid Island. There are currently three recognized subspecies of *A. expansa*, including *A. e. expansa* Bates, of China and Taiwan, *A. e. lanshuensis* Nomura of Orchid Island, and *A. e. lutaoensis* Nomura of Green Island (Yu *et al.*, 1998). The two island subspecies, *A. e. lutaoensis* and *A. e. lanshuensis*, differ subtly in their colour pattern and elytral shape (Yu *et al.*, 1998), which, similar to the case of *P. sonani*, raises the question of whether these two subspecies consist of two distinct cryptic species and of the degree of ecological divergence between them. The number of endemic species and the level of endemism in these small oceanic islands require further examination.

Supporting Information

Additional Supporting Information may be found in the online version of this article under the DOI reference:
10.1111/syen.12242

Appendix S1. Information of the specimens used in this study.

Appendix S2. GenBank accession numbers of the samples used in this study.

Appendix S3. The character coding of colour pattern in *Pachyrhynchus sonani* and outgroups.

Appendix S4. The character coding of colour pattern in *Pachyrhynchus tobafolius* and outgroups.

Appendix S5. Description of character states of colour traits in *Pachyrhynchus sonani*.

Appendix S6. Description of character states of colour traits in *Pachyrhynchus tobafolius*.

Appendix S7. Morphometric analyses of body shape between sexes based on 21 landmarks for: (a–h) *Pachyrhynchus sonani*; (i–p) *Pachyrhynchus tobaefolius*.

Appendix S8. Structure analyses of *Pachyrhynchus sonani* and *Pachyrhynchus tobaefolius*.

Appendix S9. The gene trees of *Pachyrhynchus sonani*.

Appendix S10. The *coxI* gene tree of *Pachyrhynchus tobaefolius*.

Appendix S11. The posterior probability of parameters under four gamma prior distributions in iBPP analyses.

Appendix S12. The heritability of traits under four gamma prior distributions in iBPP analyses.

Acknowledgements

We thank Cheng-Huang Lin and Pei-Jun Chen for assistance with SEM; Lu-Yi Wang, Po-Meng Chuang, Po-Sheng Liao, Yu-Wen Guo, Chang-Yi Lee, Jung-Yu Hsu and Cheng-Hsiung Chang for help with sample collection; three anonymous reviewers and Shaun Winterton for helpful comments; the High-Throughput Genome Analysis Core Facility of National Core Facility Program for Biotechnology, Taiwan (MOST 103-2319-B-010-001) for performing sequencing; and the Genome Sequencing Core of the University of Kansas for conducting RAD-seq. The Ministry of Science and Technology (MOST) of Taiwan provided financial support for this study (103-2311-B-029-001-MY3 & 104-2621-B-003-002-MY3 to C-P. Lin), and we appreciate the endangered species research permits (nos 1001700401, 1021700402, 1031700770 and 1041700842) issued by the Council of Agriculture, Taiwan. The authors have no conflict of interest to declare. There are no disputes over the ownership of the data presented in the paper. All contributions have been attributed appropriately via co-authorship or acknowledgement.

References

- Anderson, T.W. (1984) *An Introduction to Multivariate Statistical Analysis*, 2nd edn. John Wiley and Sons, Inc., Hoboken, New Jersey.
- Andolfatto, L., Lavernhe, S. & Mayer, J.R.R. (2011) Evaluation of servo, geometric and dynamic error sources on five-axis high-speed machine tool. *International Journal of Machine Tools and Manufacture*, **51**, 787–796.
- Bailey, R.C. & Byrnes, J. (1990) A new, old method for assessing measurement error in both univariate and multivariate morphometric studies. *Systematic Zoology*, **39**, 124–130.
- Barley, A.J., White, J., Diesmos, A.C. & Brown, R.M. (2013) The challenge of species delimitation at the extremes: diversification without morphological change in Philippine sun skinks. *Evolution*, **67**, 3556–3572.
- Bickford, D., Lohman, D.J., Sodhi, N.S. *et al.* (2007) Cryptic species as a window on diversity and conservation. *Trends in Ecology and Evolution*, **22**, 148–155.
- Bollino, M. & Sandel, F. (2015) Three new species of the genus *Pachyrhynchus* Germar, 1824 from Lubang Island (Philippines) (Curculionidae: Entiminae: Pachyrhynchini). *Munis Entomology & Zoology*, **22**, 392–401.
- Catchen, J., Hohenlohe, P.A., Bassham, S., Amores, A. & Cresko, W.A. (2013) Stacks: an analysis tool set for population genomics. *Molecular Ecology*, **22**, 3124–3140.
- Chang, C.E. (1986) The phylogeographical position of Botel Tobago based on the woody plants. *Journal of Phyto geography and Taxonomy*, **34**, 1–15.
- Chao, J.T., Yang, M.M. & Wu, M.H. (2009) *Setting Assessing Criteria for the Conservation of Taiwan's Threatened Insects*. Conservation Research Series No. 97–04. Council of Agriculture, Executive Yuan, Taiwan. (in Chinese).
- Coyne, J.A. & Orr, H.A. (2004) *Speciation*. Sinauer Associates Inc, Sunderland, Massachusetts.
- Darriba, D., Taboada, G.L., Doallo, R. & Posada, D. (2012) jModelTest 2: more models, new heuristics and parallel computing. *Nature Methods*, **9**, 772–772.
- Earl, D.A. & vonHoldt, B.M. (2012) STRUCTURE HARVESTER: a website and program for visualizing STRUCTURE output and implementing the Evanno method. *Conservation Genetics Resources*, **4**, 359–361.
- Edwards, D.L. & Knowles, L.L. (2014) Species detection and individual assignment in species delimitation: can integrative data increase efficacy? *Proceedings of the Royal Society of London Series B: Biological Sciences*, **281**, 20132765.
- Erbey, M. & Candan, S. (2014) The ultrastructural analysis of scales in *Brachypera Capiomont*, 1868 and *Hypera* Germar, 1817 (Coleoptera: Curculionidae: Hyperinae). *Entomological News*, **124**, 103–108.
- Falush, D., Stephens, M. & Pritchard, J.K. (2003) Inference of population structure using multilocus genotype data: linked loci and correlated allele frequencies. *Genetics*, **164**, 1567–1587.
- Felsenstein, J. (1985) Confidence limits on phylogenies: an approach using the bootstrap. *Evolution*, **39**, 783–791.
- Folmer, O., Black, M., Hoeh, W., Lutz, R. & Vrijenkoek, R. (1994) DNA primers for amplification of mitochondrial cytochrome c oxidase subunit I from diverse metazoan invertebrates. *Molecular Marine Biology and Biotechnology*, **3**, 294–299.
- Gillespie, R.G. & Roderick, G.K. (2002) Arthropods on islands: colonization, speciation, and conservation. *Annual Review of Entomology*, **47**, 595–632.
- Grant, P.R. (1998) *Evolution on Islands*. Oxford University Press, New York, New York.
- Grant, P.R. & Grant, B.R. (2014) *40 Years of Evolution: Darwin's Finches on Daphne Major Island*. Princeton University Press, Princeton, New Jersey.
- Heaney, L.R. (2000) Dynamic disequilibrium: a long-term, large-scale perspective on the equilibrium model of island biogeography. *Global Ecology and Biogeography*, **9**, 59–74.
- Hernández-Vera, G., Caldara, R., Toševski, I. & Emerson, B.C. (2013) Molecular phylogenetic analysis of archival tissue reveals the origin of a disjunct southern African–Palaeartic weevil radiation. *Journal of Biogeography*, **40**, 1348–1359.
- Hsu, Y.F. & Huang, H.C. (2008) On the discovery of *Hasora mixta limata* ssp. nov. (Lepidoptera: Hesperidae: Coeliadinae) from Lanyu, Taiwan, with observations of its unusual immature biology. *Zoological Studies*, **47**, 222–231.
- Huang, J.P. & Knowles, L.L. (2016) The species versus subspecies conundrum: quantitative delimitation from integrating multiple data types within a single Bayesian approach in Hercules beetles. *Systematic Biology*, **65**, 685–699.
- Huang, T.C. & Wu, J.T. (1998) *Flora of Taiwan*, 2nd edn. Editorial Committee of the Flora of Taiwan, Taipei.

- Kano, T. (1929) Descriptions of three new species of Curculionidae of genus *Pachyrhynchus* Germar from the island of Botel-Tobago. *The Entomological Society of Japan*, **3**, 237–238.
- Kano, T. (1933) Zoogeography of Botel Tobago Island (Kotosho) with a consideration of the northern portion of Wallace, s line. *Bulletin of the Biogeographical Society of Japan*, **9**, 381–399.
- Kano, T. (1941) Biogeography of the island of Kôtoôsho (Botel Tobago) with special reference to the New-Wallace Line. *Greater South Seas: Its Culture and Its Soil* (ed. by The Institute of the Pacific, Section of Sciences), pp. 219–323. Kawade Shobou, Tokyo.
- Kôno, H. (1930) Kurzrüssler aus dem japanischen Reich. *Journal of the Faculty of Agriculture*, **24**, 153–242.
- Lee, C.F. & Staines, C.L. (2010) *Monolepta ongi*, a new species from Lanyu Island, with redescription of its allied species *Monolepta longitarisoides* Chûjô, 1938 (Coleoptera: Chrysomelidae: Galerucinae). *Proceedings of the Entomological Society of Washington*, **112**, 530–540.
- Li, H.L. (1953) Floristic interchanges between Formosa and the Philippines. *Pacific Science*, **7**, 179–186.
- Loew, E.R., Fleishman, L.J., Foster, R.G. & Provencio, I. (2002) Visual pigments and oil droplets in diurnal lizards: a comparative study of Caribbean anoles. *Journal of Experimental Biology*, **205**, 927–938.
- Losos, J. (2009) *Lizards in an Evolutionary Tree, Ecology and Adaptive Radiation of Anoles*, Vol. **10**. University of California Press, Oakland, California.
- MacArthur, R.H. & Wilson, E.O. (1967) *The Theory of Island Biogeography*. Princeton University Press, Princeton, New Jersey.
- Mayr, E. (1995) Species, classification, and evolution. *Biodiversity and Evolution* (ed. by R. Arai, M. Kato and Y. Doi), pp. 3–122. National Science Museum Foundation, Tokyo.
- McNamara, M.E., Briggs, D.E., Orr, P.J. et al. (2013) The fossil record of insect color illuminated by maturation experiments. *Geology*, **41**, 487–490.
- Nixon, K.C. (1999) The parsimony ratchet, a new method for rapid parsimony analysis. *Cladistics*, **15**, 407–414.
- Norusis, M.J. (2005) *SPSS for Windows, v.12.0*. SPSS, Inc., Chicago, Illinois.
- Oberprieler, R.G., Marvaldi, A.E. & Anderson, R.S. (2007) Weevils, weevils, weevils everywhere. *Zootaxa*, **1668**, 491–520.
- Pellens, R. & Grandcolas, P. (eds) (2016) *Biodiversity Conservation and Phylogenetic Systematics: Preserving Our Evolutionary Heritage in an Extinction Crisis*. Springer International Publishing, New York, New York.
- Pyron, R.A., Hsieh, F.W., Lemmon, A.R., Lemmon, E.M. & Hendry, C.R. (2016) Integrating phylogenomic and morphological data to assess candidate species-delimitation models in brown and red-bellied snakes (*Storeria*). *Zoological Journal of the Linnean Society*, **177**, 937–949.
- de Queiroz, K. (2007) Species concepts and species delimitation. *Systematic Biology*, **56**, 879–886.
- de Queiroz, K. & Donoghue, M.J. (1988) Phylogenetic systematics and the species problem. *Cladistics*, **4**, 317–338.
- Rato, C., Harris, D.J., Carranza, S., Machado, L. & Perera, A. (2016) The taxonomy of the *Tarentola mauritanica* species complex (Gekkota: Phyllodactylidae): Bayesian species delimitation supports six candidate species. *Molecular Phylogenetics and Evolution*, **94**, 271–278.
- Rohlf, F.J. (2005) *tpsDig, Digitize Landmarks and Outlines, Version 2.05*. Department of Ecology and Evolution and Department of Anthropology, Stony Brook University, Stony Brook, New York.
- Rohlf, F.J. & Slice, D. (1990) Extensions of the procrustes method for the optimal superimposition of landmarks. *Systematic Zoology*, **39**, 40–59.
- Ronquist, F., Teslenko, M., van der Mark, P. et al. (2012) MrBayes 3.2: efficient Bayesian phylogenetic inference and model choice across a large model space. *Systematic Biology*, **61**, 539–542.
- Schultze, W. (1923) A monograph of the pachyrhynchid group of the Brachyderinae, Curculionidae: part I. The genus *Pachyrhynchus* Germar. *The Philippine Journal of Science*, **23**, 609–673.
- Sheets, D.H. (2004) *IMP, the Integrated Morphometric Package* [WWW document]. URL <http://www.canisius.edu/~sheets/morphsoft.ht> [accessed on 1 September 2015].
- Sikes, D.S. & Lewis, P.O. (2001) *Software Manual for PAUPRat: A Tool to Implement Parsimony Ratchet Searches Using PAUP**. Distributed by the authors [WWW document]. URL https://www.researchgate.net/publication/259239111_Software_manual_for_PAUPRat_A_tool_to_implement_Parsimony_Ratchet_searches_using_PAUP [accessed on 1 September 2015].
- Sokal, R.R. (1973) The species problem reconsidered. *Systematic Biology*, **22**, 360–374.
- Solís-Lemus, C., Knowles, L.L. & Ané, C. (2015) Bayesian species delimitation combining multiple genes and traits in a unified framework. *Evolution*, **69**, 492–507.
- Stamatakis, A. (2006) RAXML-VI-HP: maximum likelihood-based phylogenetic analyses with thousands of taxa and mixed models. *Bioinformatics*, **22**, 2688–2690.
- Starr, C.K. & Wang, H.Y. (1992) Pachyrhynchine weevils (Coleoptera: Curculionidae) of the islands fringing Taiwan. *Journal of Taiwan Museum*, **45**, 5–14.
- Swindell, S.R. & Plasterer, T.N. (1997) *SEQMAN. Sequence Data Analysis Guidebook*. Springer, New York, New York.
- Swofford, D.L. (2002) *PAUP*: Phylogenetic Analysis Using Parsimony (and Other Methods)*, v. 4.0b10. Sinauer Associates, Sunderland, Massachusetts.
- Tamura, K., Stecher, G., Peterson, D., Filipski, A. & Kumar, S. (2013) MEGA6: molecular evolutionary genetics analysis version 6.0. *Molecular Biology and Evolution*, **30**, 2725–2729.
- Tseng, H.Y., Lin, C.P., Hsu, J.Y., Pike, D.A. & Huang, W.S. (2014) The functional significance of aposematic signals: geographic variation in the responses of widespread lizard predators to colourful invertebrate prey. *PLoS ONE*, **9**, e91777.
- Wagner, W.L. & Funk, V.A. (1995) *Hawaiian Biogeography*. Smithsonian Institution Press, Washington, District of Columbia.
- Wallace, A.R. (1895) *Natural Selection and Tropical Nature: Essays on Descriptive and Theoretical Biology*. Macmillan, London.
- Weekers, P.H.H., De Jonckheere, J.F. & Dumont, H.J. (2001) Phylogenetic relationships inferred from ribosomal ITS sequences and biogeographic patterns in representatives of the genus *Calopteryx* (Insecta: Odonata) of the West Mediterranean and adjacent West European zone. *Molecular Phylogenetics and Evolution*, **20**, 89–99.
- Welch, V., Lousse, V., Deparis, O., Parker, A. & Vigneron, J.P. (2007) Orange reflection from a three-dimensional photonic crystal in the scales of the weevil *Pachyrhynchus congestus pavonius* (Curculionidae). *Physical Review E*, **75**, 041919.
- Wheeler, Q.D., Knapp, S., Stevenson, D.W. et al. (2012) Mapping the biosphere: exploring species to understand the origin, organization and sustainability of biodiversity. *Systematics and Biodiversity*, **10**, 1–20.
- Whittaker, R.J., Triantis, K.A. & Ladle, R.J. (2008) A general dynamic theory of oceanic island biogeography. *Journal of Biogeography*, **35**, 977–994.
- Wiens, J.J. (2007) Species delimitation: new approaches for discovering diversity. *Systematic Biology*, **56**, 875–878.
- Wiley, E.O. (1978) The evolutionary species concept reconsidered. *Systematic Biology*, **27**, 17–26.

- Yang, Z. & Rannala, B. (2010) Bayesian species delimitation using multilocus sequence data. *Proceedings of the National Academy of Sciences of the United States of America*, **107**, 9264–9269.
- Yang, T.F., Lee, T., Chen, C.H., Cheng, S.N., Knittel, U., Punongbayan, R.S. & Rasdas, A.R. (1996) A double island arc between Taiwan and Luzon: consequence of ridge subduction. *Tectonophysics*, **258**, 85–101.
- Yen, S.H., Kitching, I.J. & Tzen, C.S. (2003) A new subspecies of hawkmoth from Lanyu, Taiwan, with a revised and annotated checklist of the Taiwanese Sphingidae (Lepidoptera). *Zoological Studies*, **42**, 292–306.
- Yewers, M.S., McLean, C.A., Moussalli, A., Stuart-Fox, D., Bennett, A.T.D. & Knott, B. (2015) Spectral sensitivity of cone photoreceptors and opsin expression in two colour-divergent lineages of the lizard *Ctenophorus decresii*. *Journal of Experimental Biology*, **218**, 1556–1563.
- Yoshida, H., Tso, I.M. & Severinghaus, L. (2000) The spider family Theridiidae (Arachnida: Araneae) from Orchid Island, Taiwan: descriptions of six new and one newly recorded species. *Zoological Studies*, **39**, 123–132.
- Yoshitake, H. (2012) Nine new species of genus *Pachrhynchus* Germar (Coleoptera: Curculionidae) from the Philippines. *Esakia*, **52**, 17–34.
- Yu, C.J., Chu, Y.I. & Kobayashi, H. (1998) *The Scarabaeidae of Taiwan*. Mu Sheng Press, Taipei.
- Zhang, C., Zhang, D.X., Zhu, T. & Yang, Z. (2011) Evaluation of a Bayesian coalescent method of species delimitation. *Systematic Biology*, **60**, 747–761.

Accepted 1 May 2017